Nuclear Engineering and Technology 53 (2021) 484–497

Contents lists available at ScienceDirect

Nuclear Engineering and Technology

journal homepage: www.elsevier.com/locate/net

Original Article

Time uncertainty analysis method for level 2 human reliability analysis of severe accident management strategies

Young A Suh, Jaewhan Kim*, Soo Yong Park

Korea Atomic Energy Research Institute, Yuseong, Daejeon, 305-600, South Korea

ARTICLE INFO

Article history:
Received 8 May 2020
Received in revised form
22 June 2020
Accepted 21 July 2020
Available online 29 July 2020

Keywords:
Level 2 human reliability analysis
Severe accident management guideline
Time uncertainty analysis
Sums of lognormal distributions
Total loss of component cooling water (TLOCCW)

ABSTRACT

This paper proposes an extended time uncertainty analysis approach in Level 2 human reliability analysis (HRA) considering severe accident management (SAM) strategies. The method is a time-based model that classifies two time distribution functions—time required and time available—to calculate human failure probabilities from delayed action when implementing SAM strategies. The time required function can be obtained by the combination of four time factors: 1) time for diagnosis and decision by the technical support center (TSC) for a given strategy, 2) time for strategy implementation mainly by the local emergency response organization (ERO), 3) time to verify the effectiveness of the strategy and 4) time for portable equipment transport and installation. This function can vary depending on the given scenario and includes a summation of lognormal distributions and a choice regarding shifting the distribution. The time available function can be obtained via thermal-hydraulic code simulation (MAAP 5.03). The proposed approach was applied to assess SAM strategies that use portable equipment and safety depressurization system valves in a total loss of component cooling water event that could cause reactor vessel failure. The results from the proposed method are more realistic (i.e., not conservative) than other existing methods in evaluating SAM strategies involving the use of portable equipment.

1. Introduction

Humans play an important role in both maintaining safe operation and mitigating accident situations in nuclear power plants (NPPs) [1,2]. For realistic assessments of plant safety, human reliability analysis (HRA) is an essential aspect of probabilistic safety assessment (PSA) [3]. As part of the enhanced defense-in-depth strategies currently being developed for NPPs following the Fukushima accident, severe accident management guidelines (SAMGs) have been revised with the introduction of portable equipment, which are used as primary means in overall strategies for coping with beyond design basis events (BDBEs) such as diverse and flexible coping strategies (FLEX) or multi-barrier accident coping strategies (MACST) [4]. However, current HRA approaches have not considered how SAMGs will progress with FLEX/MACST equipment, and moreover, current HRAs have limitations in reflecting SAMG action characteristics after the onset of core damage. The modeling of SAMG actions for Level 2 HRA needs to take into account the following significant features: phenomenological uncertainties about the plant state, timing of entry into SAMGs and possible delays in composing the emergency response organization (ERO) affecting readiness for accident mitigation, and coordination between multiple teams [5–7]. Additionally, the timing of portable equipment transport and installation has now become essential. Thus, a new approach is necessary to evaluate SAMG HRA to reflect FLEX/MACST strategy. This paper focuses on a time-based model among the late-developing detailed Level 2 HRA methodologies [8].

As cognitive research has demonstrated that human errors increase in time-constrained conditions [9], a variety of time-based models have been developed in the past decades to reflect the importance of timing issues. The models include the human cognitive reliability (HCR) method [10,11], the HCR and operator reliability experiments (OREs) [12,13] by the Electric Power Research Institute (EPRI) [14], Kim and Ha's method [15], and the integrated human event analysis system (IDHEAS) [16]. The HCR and HCR/ORE methods focus on cognitive processing in Level 1 situations. The Kim and Ha method proposed a time model for severe accidents that considers phenomenological uncertainties, which is similar to the Level 2 scope of the present work. The

* Corresponding author.
E-mail addresses: sya@kaeri.re.kr (Y.A. Suh), jhkim4@kaeri.re.kr (J. Kim), sypark@kaeri.re.kr (S.Y. Park).

https://doi.org/10.1016/j.net.2020.07.028

IDHEAS method is the latest and most generic approach, in which human failure probability (HFP) is quantified by the summation of the error probabilities attributed to failures in macro cognitive functions and failures due to time uncertainty.

Existing time-based models are insufficient in modeling time uncertainty for assessing severe accident management (SAM) strategies, which are characterized by phenomenological uncertainty and involvement of various tasks and actors. For example, the available time for a human action in a Level 1 PSA is used in a best-estimate point value, but for Level 2 PSA it is necessary to consider phenomenological uncertainty in estimating a time limit for a SAM measure. For SAM strategies, the evaluation should consider involvement of various tasks and actions, which are conducted by a different ERO, in estimating a total required time taken for completing a SAM measure. Those tasks and actions include diagnosis and decision of a strategy by the TSC, implementation of the strategy by the coordinated activity between the MCR crew and the local EROs, including transport and installation of portable equipment, verification of the effectiveness of the strategy, and so on.

The objective of this paper is to propose an extended approach to time analysis to reflect SAM strategies including FLEX/MACST equipment for Level 2 HRA. The method classifies two time distribution functions for calculating HFP due to a delayed action: time required and time available functions. It uses a stochastic and sequential approach to resolve timing problems regarding SAMG action and system operation by the TSC. The extended approach involves the following steps: 1) run thermal-hydraulic simulations (MAAP 5.03) to obtain a distribution of time available reflecting phenomenological uncertainty; 2a) collect the SAMG performance time data to obtain the distributions of time required; for our study the data collected from table top exercises (TTXs) and stress tests were used; 2b) fit the data to find a suitable distribution; 2c) integrate the distributions; and 3) calculate HFP due to a delayed action from mathematical integration. The developed approach was applied to assess a SAM strategy that employ portable equipment in a total loss of component cooling water (TLOCCW), an event that has the potential to lead to reactor vessel (RV) failure. An uncertainty analysis for finding an appropriate sigma value was added to reflect the uncertainty caused by the various statistical processes. A sensitivity analysis was also conducted to see the impact of degraded and stressful conditions in severe accidents and to validate the difference between simulation and actual values. The paper concludes with comparisons between the results from the proposed approach and the conventional point estimation approach, along with related discussions.

2. Methodology

The proposed method is an extension of the time-based model that convolutes two time distribution functions for calculating HFP due to a delayed action: time required ($T_{required}$) and time available ($T_{available}$).

In the real world, the time required to perform the actions in a human failure event should be represented with a probability distribution function to capture related uncertainties. In addition, this methodology includes all cognitive and physical performance (execution actions) times in calculating time required, since all tasks utilize cognitive activities and physical human activities must be performed within the final available time to complete all of the given tasks. Thus, $T_{required}$ represents the time taken for the actions in accident mitigation, which includes conducting each SAG (i.e., diagnosing and judging whether or not to implement a given SAG, executing the action in the SAG, and verifying the effectiveness of the strategy) and deploying and installing portable equipment based on the SAMG entry point.

Evaluation of SAMG strategies requires basic time information based on severe accident analysis and the response from various emergency organizations. As the most basic information, the timing of SAMG entry ($T_{SAMG\text{-}CET@650}$) should be identified for the scenarios to be analyzed, as well as the time of emergency alert for each of emergency response organizations (ERO) according to the Emergency Plan (EP) of the NPP. In the event of an emergency situation, several EROs are called for such as the TSC, the operator support center, the emergency operator facility, and MACST-operating organizations. The time between the ERO being called for and their being ready for conducting emergency response should also be estimated. The actual time required to start and operate an ERO may be affected by a number of factors, including the presence and severity of natural disasters, the time of emergency alert, the place of residence of workers, the route and methods of travel, and weather conditions. In this study, the possibility of injury or damage to ERO personnel is ignored by assuming a general design basis event situation (rather than an extreme natural disaster situation), with the time required for the ERO to move and launch on-site after emergency issuance assumed to be about 2 h. Of course, if more detailed time information related to the launch of a well-founded ERO can be collected, that information can be applied.

After SAMG entry, specific time information related to SAMG progress and strategy implementation is also required. Such time information includes the time from SAMG entry to the time of initial implementation of the SAMG diagnosis flowchart, the time of judgment and decision-making in each SAG, the completion of the given strategies using portable equipment including on-site actions, and the time required to verify the effectiveness of the strategy implementation and to terminate each SAG.

The overall time required should be evaluated as a holistic integration of all the individual time information obtained. Here, time information is not just point estimation values, but takes the form of probability distributions that contain each of the unique task characteristics; therefore, a systematic process of integrating the individual time information is necessary. In general, assuming operator actions are approximated as lognormal distributions in PSA/HRA, the integration of lognormal distributions should be calculated in order to produce an overall time distribution from the individual time distributions. In the absence of accurate simulator data of SAG implementation and verification, shifting the lognormal distributions should also be applied to add to this assumed value (in the form of a point value).

In order to integrate individual time information, the data obtained should first be verified for suitability to lognormal distribution, after which the integration of lognormal distributions can be obtained. However, the summation process is not easier than lognormal multiplication, since accurate mathematical methods have yet to be shown; there are only ways to estimate approximations of lognormal sums. Thus, this study sought to obtain consensus approximation using the moment generating function of the two distributions, with Monte Carlo sampling of the lognormal distributions used to simulate a new consensus distribution. We also used the three-parameter lognormal method (referred to here as Approach 1) to add a few assumed time values to the obtained consensus distribution. As an alternative approach, we simply added the logarithmic mean of the consensus distribution to a few assumed time values while maintaining the original sigma value of the distribution (referred to here as Approach 2). Detailed methods are described in the case analysis.

Similarly, because of the various uncertainties associated with systems or structures (e.g., RV or containment integrity), the time available ($T_{available}$) for the implementation of given strategies should also be described with a probability distribution function.

For example, the RV failure probability may differ depending on the time to transport portable equipment or the point of coolant injection and strategies taken. In short, $T_{available}$ represents the time available to conduct given strategies while maintaining intact systems or structures.

Our method proposes to calculate the HFP due to a delayed action (P_{Fr}) that occurs when the time required exceeds the time available. Here, P_{Fr} represents the probability that the TSC fails in implementing the SAM strategies to mitigate irreversible plant states (RV failure or containment failure). The P_{Fr} term is the convolution of the probability density functions of $T_{available}$ and $T_{required}$, and can be obtained as follows:

$$P_{Fr} = Probability\left(T_{required} > T_{available}\right) = \int_0^\infty f_{T_{available}}(t) \cdot \left[1 - F_{T_{required}}(t)\right] dt = \int_0^\infty f_{T_{required}}(t) \cdot F_{T_{available}}(t)\, dt, \quad (1)$$

where $F_{T_{required}}(t)$ and $F_{T_{available}}(t)$ are the cumulative distribution functions of $T_{required}$ and $T_{available}$, and $f_{T_{required}}(t)$ and $f_{T_{available}}(t)$ are the probability density functions of $T_{required}$ and $T_{available}$.

Fig. 1 shows how P_{Fr} can be calculated between the two probability density functions. In the figure, P_{Fr} corresponds to the two diagonal sets of lines [slash (/) and inverse slash (\)]. In the plot, although the mean value of $T_{available}$ is significantly greater than that of $T_{required}$, there is still error probability as indicated in the shaded area due to the overlapping tails of the two probability density functions. For comparison with the point estimation method, Fig. 1 also illustrates P_{Fr} corresponding to the diagonal lines (slashed). Detailed examples for better understanding will be provided in following sections.

The application of our model into SAMG HRA needs to take into account the following significant features: phenomenological uncertainties about the plant state, the timing of SAMG entry and possible ERO delays, and the required coordination of multiple teams. Additionally, the time of portable equipment transport and installation is essential to model SAMG HRA to include FLEX/MACST equipment. To consider these various factors in our model, the first step for time analysis evaluation is developing a scenario timeline that is both detailed and plant specific. According to Kirwan and Ainsworth (1992) [17], the development of a realistic timeline provides a key focal point for related PSA models. A description of the event scenario timing and functional success criteria can clarify the modeled actions and illustrate how multiple actions during an integrated scenario interact with each other (e.g., sequentially, in parallel, partially overlapping in time, etc.).

Depending on the scenario, accident sequence, and plant-specific situation, several timelines can be developed for one initiating event. Thus, timelines can change even in the same accident depending on external environmental factors. For example, considering a TLOCCW event, the time required will be extended if the cause is from extreme or high-damage external factors rather than lower damage external events. This paper therefore focuses on design basis events (DBEs) that lead to SAMG entry. It is also assumed that only portable pumps are available for steam generator (SG) or reactor coolant system (RCS) injection for accident mitigation. The patterns of strategy implementations in response to an accident can be categorized into four cases, as shown in Fig. 2.

The terms associated with each timing element are defined as below.

- *Event* = A design basis initiating event that leads to reactor trip.
- $T_{ERO_{ready}}$ = ERO ready time. Time at which each of the EROs is functional or ready to give guidance or implement the requested actions once the emergency alert is made, including the time taken to travel and be ready to initiate the required mission. This time may differ between EROs.
- *Emergency alert time* = Time at which the emergency alert is requested or issued for calling the ERO to the site based on the EP of the site. The EROs include the TSC emergency staff, the emergency operator facility, the operator support center, and the local emergency staff responsible for deploying and installing the portable equipment.
- $T_{SAMG\ Entry\ condition}$ = Time at which the SAMG entry condition is reached (e.g., core exit temperature (CET) is 650 °C and rising in the reference plant). This time information can be obtained from accident analysis code.
- $T_{Transport\ and\ intallation}$ = Time required to deploy and install the portable equipment.
- $T_{SAG\#}$ (Time for SAG-#) = Time required for conducting each SAG, including the time for system identification, decision-making in the strategy, direction to the implementers (e.g., MCR crew or local personnel), and monitoring the effectiveness of the strategy. This time may differ for each SAG. This term is categorized into $T_{SAG\#\_d}$, $T_{SAG\#\_a}$, and $T_{SAG\#\_v}$, as follows.
  - $T_{SAG\#\_d}$: Time for SAG diagnosis and decision-making.
  - $T_{SAG\#\_a}$: Time for SAG action (implementation).
  - $T_{SAG\#\_v}$: Time for the verification of SAG effectiveness.

At the SAMG entry point, the TSC usually receives information from the MCR to make a decision on which strategy should be selected, and how and when the strategy should be implemented. Related actions are then taken in a timely manner before the plant reaches an irreversible state (e.g., RV or containment failure).

- **Case 1** represents that the transport and installation of the portable equipment happened prior to SAMG entry, so that the

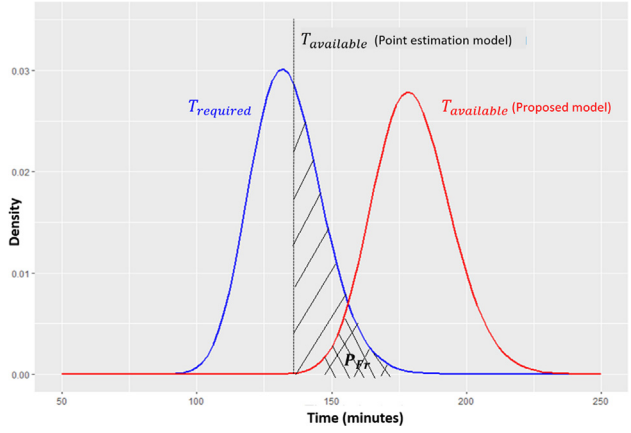

Fig. 1. Proposed model compared to point estimation model.

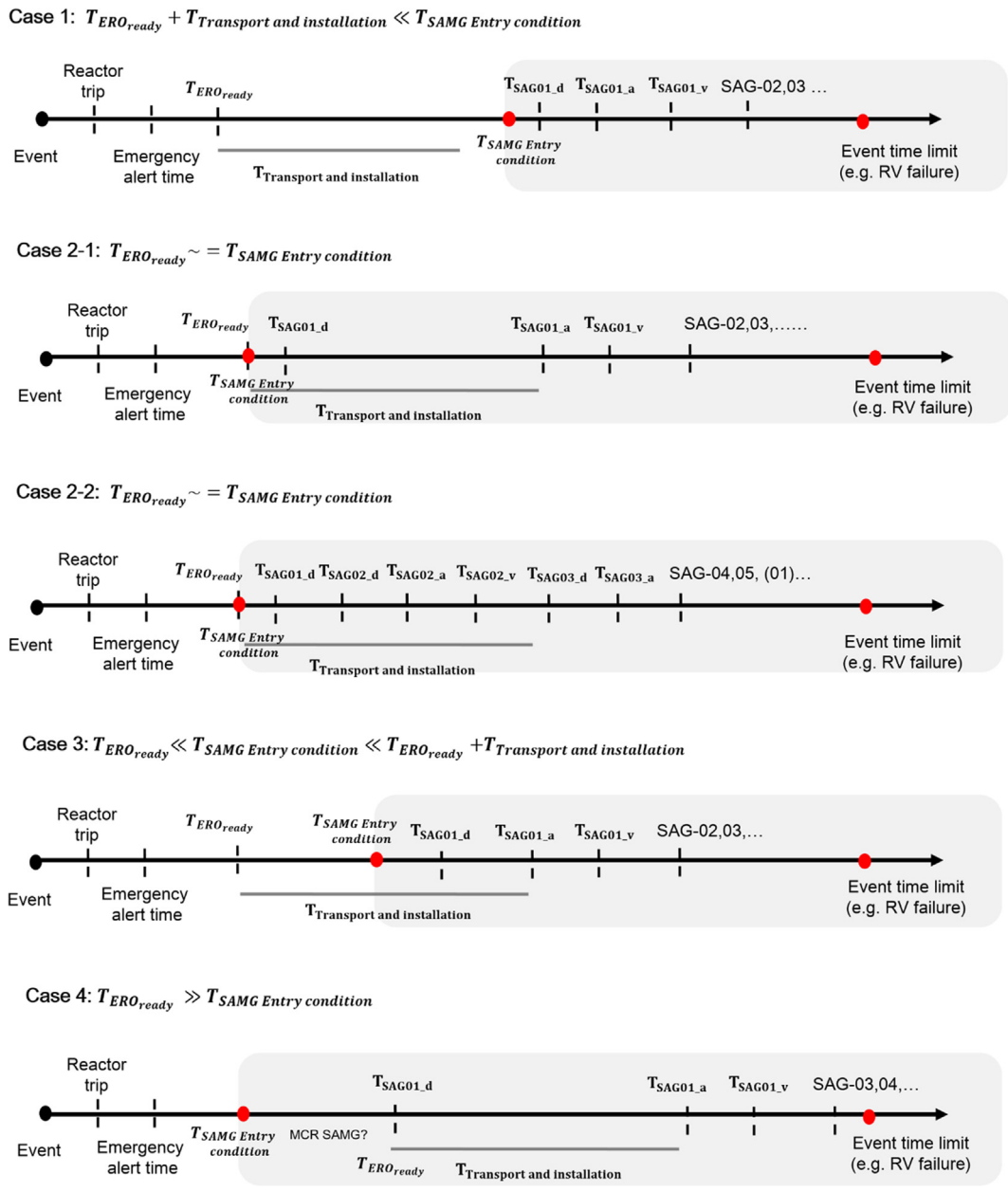

Fig. 2. Timelines for representing various cases of SAG implementation. (The gray shaded areas are the focus of the current work.)

equipment is in standby mode at the SAMG entry point (or when performing SAG-1). In this case, SAG decisions regarding the use of portable equipment and the implementation of the SAGs can be made at the proper time.

- **Case 2-1** represents that the ERO ready time is similar to the SAMG entry time; in this case, the SAG actions on using portable equipment will be delayed until transport and installation is completed. Here, the time to SAG-2 is too late, assuming that it is performed sequentially from SAG-1. In this case, SAG-2 may be implemented first, which is RCS depressurization using the safety depressurization system (SDS); this situation is represented by **Case 2-2,** in which SAG-2 starts after only SAG-1 situational judgment and decision was completed but before SAG-1 implementation, considering the time required.
- **Case 3** represents that the transport of the portable equipment had been initiated before SAMG entry, but the SAMG entry is rapid and the deployment is still in motion. If the equipment is in transport, implementation of SAG-1 in this case is expected to be nearly similar to Case 2-1. On the other hand, if the equipment is in deployment, the TSC may be confused whether to first implement SAG-2 or to first wait until the equipment is fully deployed; if performed after SAG-2, this case would be similar to Case 2-2 and therefore a preliminary analysis of the case waiting for full deployment (Case 3) can be performed.
- **Case 4** represents an extreme or high-damage external event in which the ERO and the installation of portable equipment to enter SAMG is late. Here, the SAMG entry condition is reached before the ERO is configured, and in this case, MCR SAMG (e.g., severe accident control room guidance (SACRG)) might be performed. While current SACRG does not include actions using portable equipment, RCS depressurization strategies such as the opening of the SDS are included.

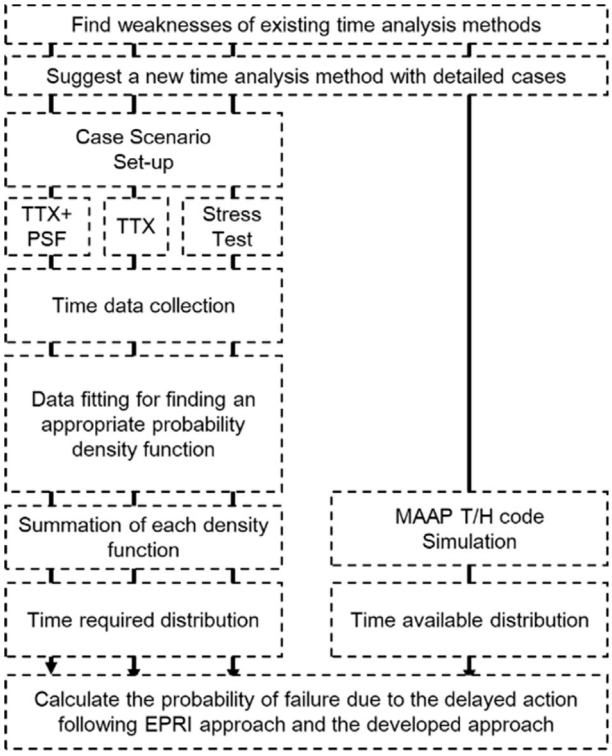

Fig. 3. Research approach to developing the time analysis method.

Taking into account the above SAMG time-related characteristics, a calculation approach to P_{Fr} can be created, as shown in Fig. 3. Here, time required distribution refers to the time when the implementation of a given strategy is completed, including portable equipment transportation and deployment, and time available distribution refers to the success criterion of the system or structure integrity. Following this approach, application results of the TLOCCW case are described in the next section.

3. Application: case studies

The proposed method was applied to evaluate SAG strategies for preventing RV failure in a TLOCCW accident in the OPR1000 which is a Korean domestic NPP. This section includes the following steps: 1) develop timelines of the case studies, 2) calculate the time required distribution using data collection and statistical analysis, 3) identify the time available using MAAP 5.03 code, 4) compare the results between our method and the point estimation method, 5) conduct a sigma uncertainty analysis, and 6) perform a sensitivity analysis considering three types of PSFs.

3.1. Case study timelines

A TLOCCW is initiated with the success of a reactor trip. However, a loss of the secondary heat removal function then occurs due to the failure to deliver auxiliary feedwater using turbine-driven and motor-driven pumps. Operators then decide whether to conduct the feed-and-bleed (F&B) operation within 2 h. The decision to not perform the F&B operation means that the RCS can be maintained at high pressure. As the high-pressure safety injection (HPSI) pumps can fail at an early stage due to the loss of room cooling induced by TLOCCW, portable pumps are expected to be used as SAM measures for injecting coolant to the SGs and RCS. The underlying assumptions in this scenario are as follows: 1) containment pressure is stable, 2) instrumentation and control (I&C) systems and the integrity of the communication devices between the TSC and MCR are not affected by the TLOCCW event, and 3) external disasters such as an earthquake or tsunami are not considered. Fig. 4 describes the detailed scenario using a PDS-ET (plant damage state–event tree).

Following this scenario, SAG-01, SAG-02, SAG-03, and SAG-06 among the seven SAGs are associated with the TLOCCW event, based on the SAMG diagnosis flow chart in Fig. 5. In this event, first, SG water levels are not sufficient to satisfy the criteria, and thus injection into the SGs (SAG-01) should be considered. Since the F&B operation fails in the EOP regime, SAG-02 is then considered for mitigating the accident. These cases are called “RCS high pressure”. Since the CET is above the criteria (CET_T), injection to the RCS (SAG-03) using portable pumps can be considered as a candidate strategy. Here, SAG-4 is not considered because RCS injection using a portable pump is expected to be successful for core cooling, and SAG-05 is not applicable in this case because of no fission product release. While SAG-06 should be considered as a candidate accident management strategy, the scope of this paper focuses on the perseverance of RV integrity, and therefore SAG-06 is excluded. SAG-07 is not applicable as hydrogen is assumed to be under normal control.

In this situation, the time limit for preventing an irreversible state of the NPP can be considered as RV failure, so RV failure probability depending on time is used as one element for calculating the time available for the TSC to implement the given strategy. As described in Section 2.2, one scenario can be divided into four cases depending on $T_{ERO_{ready}}$, $T_{SAMG\ Entry\ condition}$, and $T_{Transport\ and\ intallation}$. Based on thermal-hydraulic simulation, $T_{SAMG\ Entry\ condition}$ is expected to be 2.5 h in RCS high pressure cases. This case study applies this time to the timelines in Fig. 2. Cases 3 and 4 are not included in this application since a TLOCCW with loss of secondary heat removal event under normal conditions is considered. Even though the FLEX/MACST strategy was first introduced for use in beyond design basis external events, the industry [19] has extended the application of FLEX/MACST equipment to realize cost-benefits and general safety improvement in NPPs. This scenario was developed with deliberation of the use of portable equipment, and thus only timeline Cases 1, 2-1, and 2-2 were applied to the RCS high pressure cases; detailed timelines are shown in Fig. 6.

3.2. Distribution of time required

For calculating the total time required distribution, the failure mechanism in implementing a given strategy can be influenced by four possible time states: 1) TSC diagnosis time for each strategy, 2) ERO action time (implementing SAG strategies), 3) time to verify the effectiveness of the strategy, and 4) portable equipment transport and installation time.

Based on the timelines in Fig. 6, to develop a time analysis, data collection related to time required is needed. There are various data collection methods, such as interviews, questionnaires, and observations. In this paper, we used the TTX method and data from stress tests. A total of five TSC candidates (one SAMG developer, one current TSC staff member, and three retired operators) participated in the TTX as experimental subjects from whom the time data for implementing SAGs were collected. Time data for portable equipment transport and installation were acquired from Korea Hydro & Nuclear Power stress tests.

Typically, a TTX is used as a disaster preparedness activity that takes participants through the process of dealing with a simulated disaster scenario. The TSC’s overall response in an SAMG situation cannot be perfectly imitated since it would be a dynamic situation

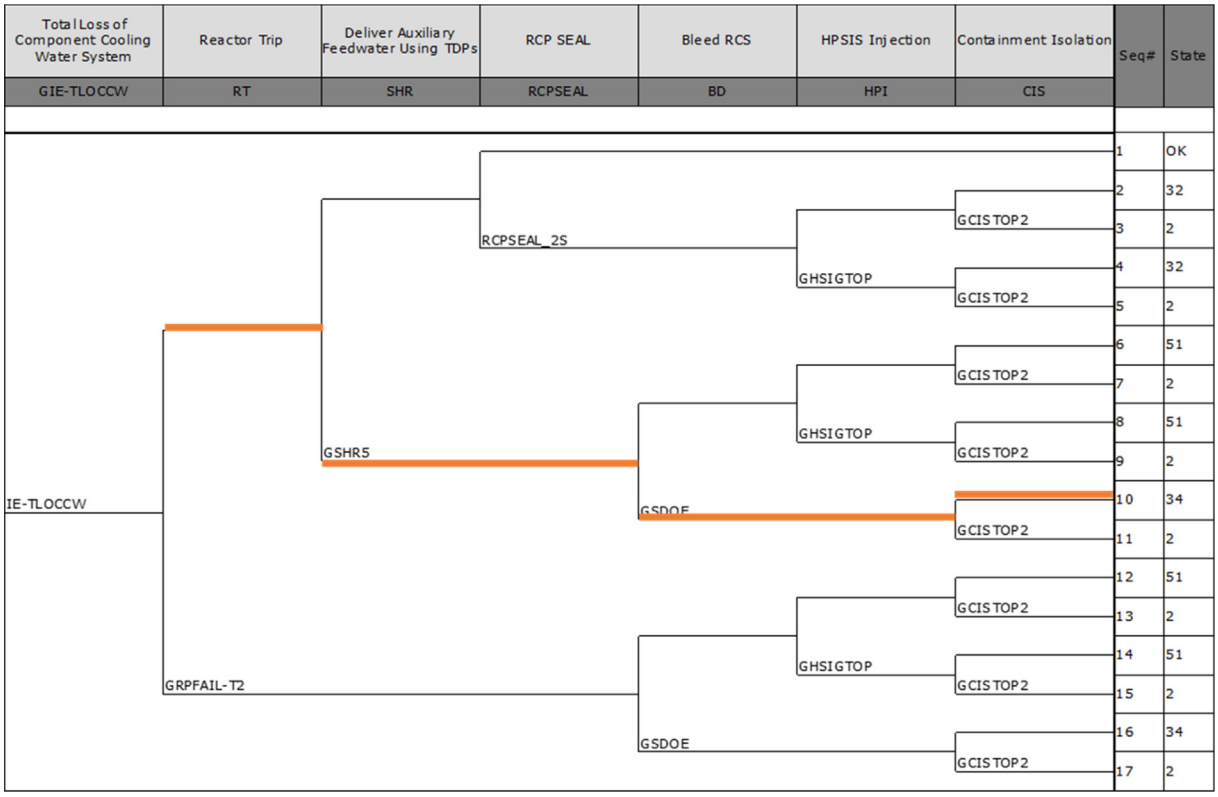

Fig. 4. Detailed scenario description of TLOCCW.

with various factors (e.g., extreme stress or dire environmental conditions); full-scale exercises are accordingly impossible due to the cost and fundamental differences between real and experimental situations. In this regard, TTXs can be useful to estimate the response time of TSC diagnosis as close to a real situation as possible, because TSC diagnosis and strategy decisions are based on SAMGs. On the other hand, SAMG implementation time includes the time to connect or manipulate equipment or components such as valves, so it is difficult to estimate implementation time or the time to verify the effectiveness of strategies by TTX. These times are therefore obtained via thermal-hydraulic analysis. To collect data on the time required to deploy and install portable equipment, this paper used stress tests. In a stress test, drills involving portable equipment are performed focusing on one specific function (time required) and process that can be tested, possibly in real-time, with real FLEX/MACST staff at Korean NPP sites.

Since the time data collected from TTXs and stress tests are in the form of simulator data, the distributions are expected to follow lognormal distribution patterns. This fact was revealed by previous HCR/ORE studies. Lognormal distribution is also important in the description of natural phenomena and human behavior [20]. However, due to the small number of data samples, it was necessary here to establish a statistical basis that the collected data followed a lognormal distribution in order to calculate time reliability. In this study, the time of SAG diagnosis from among the whole process (SAMG entry condition to SAG strategy implementation) was extracted from the TTX data. The time required for portable equipment transportation and installation was extracted from the database of the Korean OPR1000 stress tests. Based on the collected data, a statistical analysis was performed for data fitting (extrapolation) [21], a process necessary for finding the appropriate probability density function. In detail, maximum likelihood was used as the fitting method.

To find the best distribution (between normal and lognormal distribution) for the extracted time data, statistical suitability tests of the distribution were performed in parallel with the numbers following Akaike information criterion (AIC), Bayesian information criterion (BIC), and graph diagnostic methods for the results of the conformity of the distribution as shown in Fig. 7. Information criterion is a method that reflects the loss (penalty) of a number of independent variables in maximum likelihood; AIC and BIC are commonly used for the comparison of models [22]. The lower value between AIC and BIC represents the better model since it means a smaller loss of information. From the TTX and stress-test data, results of the conformity of the distribution are shown in Table 1. The best representation of the time required is the logarithmic distribution, with example plots of time required for $T_{Transport\ and\ intallation}$ shown in Fig. 7.

Sigma values (σ) of the logarithmic distribution representing variability in TSC diagnosis time were also extracted from the TTX data. Considering the uncertainty and small number of data, sigma values were predicted through applying different models for calculating the lognormal summation. A basic approach is to apply the PWR sigma values from the HCR/ORE report [9], in which average values are 0.57 (CP1), 0.38 (CP2), and 0.77 (CP3). In the SAMG situation in this application, various procedure-based human interaction categories exist, so this paper considers all three types of sigma.

As an alternative method to estimate sigma, the integration of the lognormal distributions can be used, but there is no exact method to calculate the summation of lognormal distributions. Although the summation of lognormals does not follow lognormal

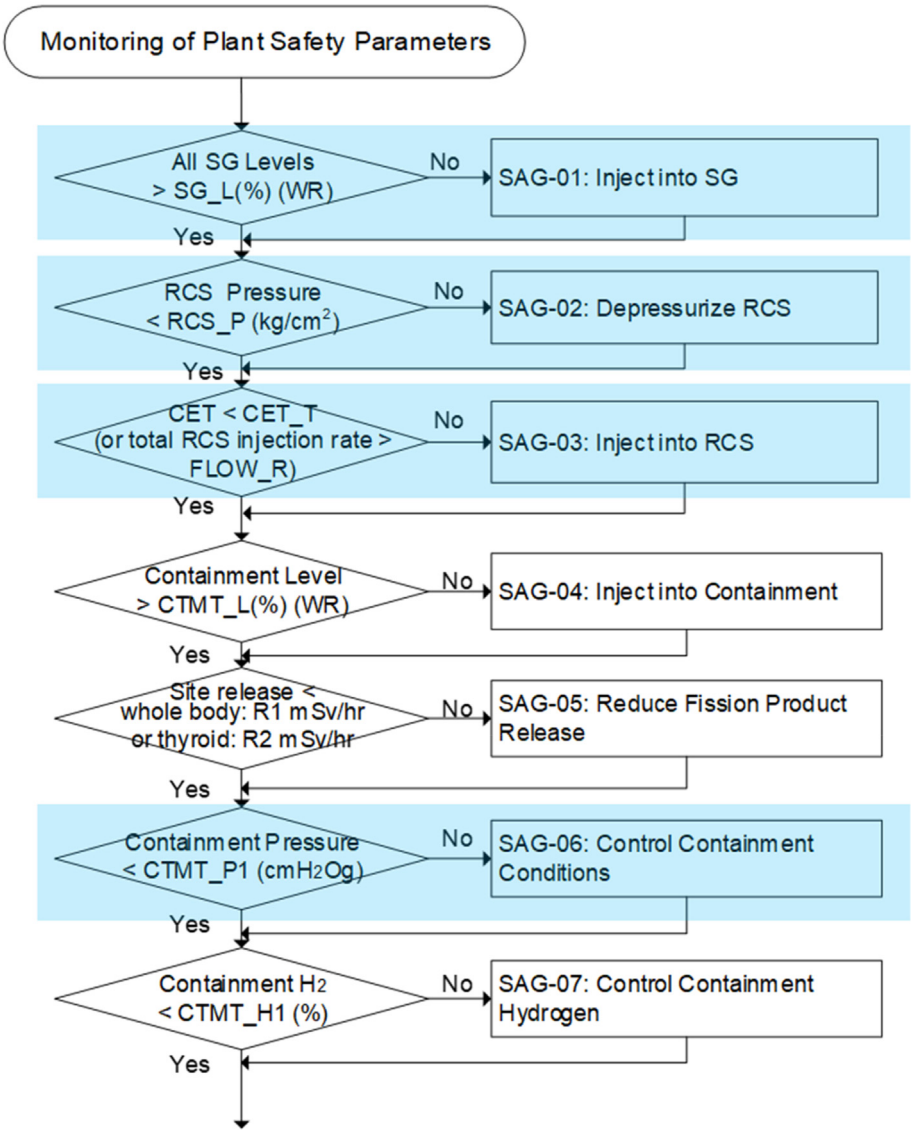

Fig. 5. Example SAMG diagnosis flow chart [18]. (The blue highlighted steps refer to the implementation of SAGs after a TLOCCW occurs). (For interpretation of the references to colour in this figure legend, the reader is referred to the Web version of this article.)

distribution, it can be reasonably approximated by another lognormal distribution only at the right tail [23,24]. The right tail is important to estimate sigma, so this paper assumes the integration of lognormals followed another form of lognormals. Because exact closed-form expressions for the lognormal summation of probability distribution functions are unknown [25], two types of analytical approximation methods can be used for estimating the sum of lognormal distributions, namely, moment-generating function matching and the Monte Carlo (MC) process using least squares fitting. To accurately estimate the sums of the lognormal distributions, this paper compared the results of applying the Fenton–Williamson (FW) technique, which is known as a moment-generating function method [26,27], with the results from the MC method, which is a computation method [28,29]. The latter was simulated by R simulation code [30]. In the FW technique, a commonly used approximation can be mathematically obtained by matching the mean and variance of another lognormal distribution as follows:

$$\sigma_Z^2 = \ln\left[\frac{\sum e^{2\mu_j+\sigma_j^2}\left(e^{\sigma_j^2}-1\right)}{\left(\sum e^{\mu_j+\frac{\sigma_j^2}{2}}\right)^2}+1\right], \quad \mu_Z = ln\left[\sum e^{\mu_j+\frac{\sigma_j^2}{2}}\right]-\frac{\sigma_Z^2}{2}, \tag{2}$$

where $X_j \sim Lognormal(\mu_j, \sigma_j^2)$ is an independent, lognormally distributed variable with possibly varying σ and μ parameters, and $Z = \sum_{j=1}^{n} X_j$.

Both methods, i.e. the MC and FW methods, have been tested for their accuracy for integrating the individual times taken for SAG-1 and SAG-3 into a summated lognormal distribution. The result shows a similar pattern between two methods, especially almost

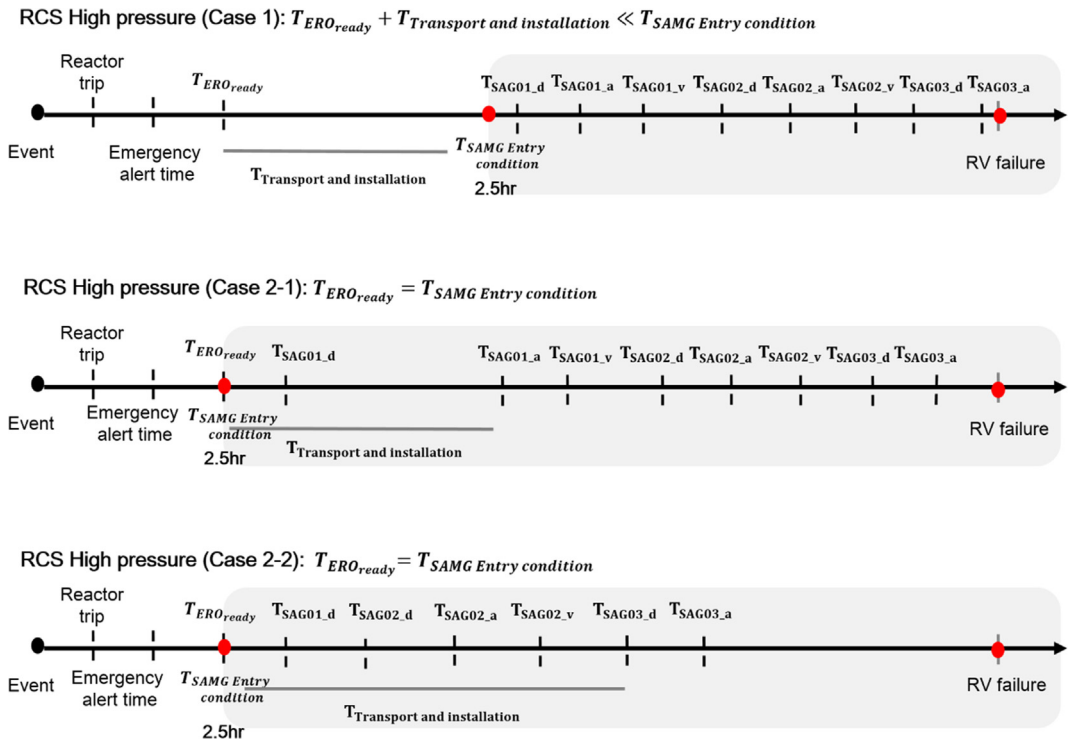

Fig. 6. Timelines of the case scenarios for time analysis development.

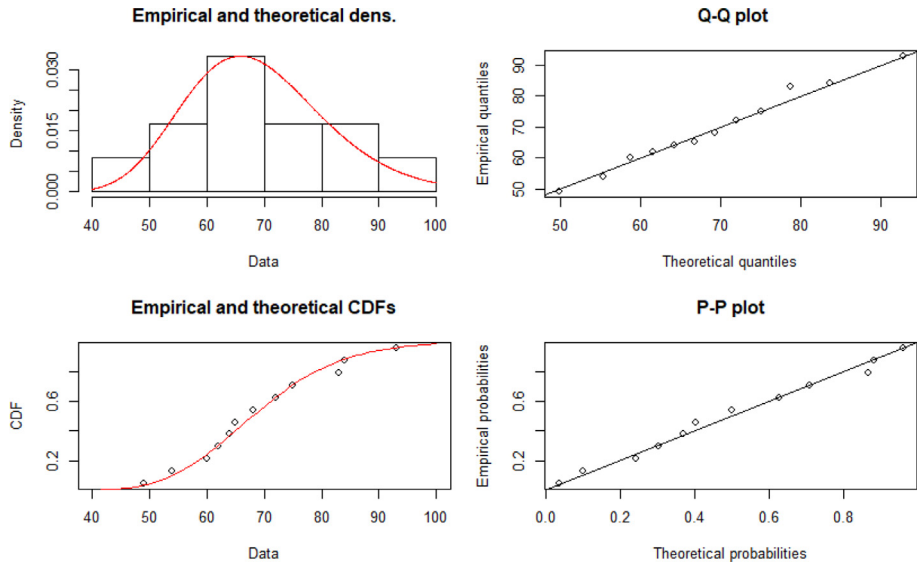

Fig. 7. Diagnosis of logarithmic distribution suitability for time required for $T_{Transport\ and\ intallation}$.

same pattern in the tail part of the summated (i.e., integrated) lognormal distribution, as shown in Fig. 8. In our study, the MC method is adopted between two methods because the one gives more accurate result and is simple to use than the FW method.

Another problem related to the estimation of total time required is shifting the lognormal distributions. Data collected by TTX only represents the SAG diagnosis and decision time ($T_{SAG\#_d}$), but implementing the SAG strategies ($T_{SAG\#_a}$) and verifying their effectiveness ($T_{SAG\#_v}$) also need to be included in the total time required (see Section 2.2). These times were assumed based on thermal-hydraulic code results with engineering judgement, and are not in the form of a distribution but rather point values. This paper assumed the data as T_{SAG01_a} = 20 min, T_{SAG01_v} = 50 min, T_{SAG02_a} = 10 min, T_{SAG02_v} = 10 min, andT_{SAG03_a} = 20 min. Thus, the SAG diagnosis and decision time ($T_{SAG\#_d}$) in lognormal distribution as represented from TTX data should be shifted by the time required for implementing and verifying each SAG.

To consider shifted lognormals, two models were developed here for calculating total HFP. Approach 1 uses the mathematical theory of three-parameter lognormals, which is a general skew distribution in which the logarithm of any linear function of a given variable is normally distributed [31–33]. When using this method,

Table 1
Goodness-of-fit tests for time required distribution models.

SAG-01 data fitting	Lognormal	Normal
Akaike's Information Criterion (AIC)	36.10	811.14
Bayesian Information Criterion (BIC)	35.32	815.93
SAG-02 data fitting		
Akaike's Information Criterion (AIC)	16.77	811.14
Bayesian Information Criterion (BIC)	14.16	815.92
SAG-03 data fitting		
Akaike's Information Criterion(AIC)	45.94	811.14
Bayesian Information Criterion (BIC)	45.16469	815.92
Portable equipment transport and installation data fitting		
Akaike's Information Criterion (AIC)	98.06	811.14
Bayesian Information Criterion (BIC)	99.03	815.92

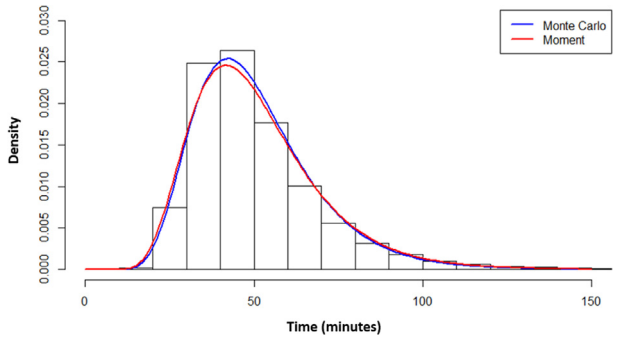

Fig. 8. Comparison of different summation methods for SAG-01 and SAG-03.

the form of the distribution is maintained, but as depicted in Fig. 9, sigma decreases. According the EPRI report [9], the logarithmic sigma is an important element for calculating the failure probability of delayed SAG implementation. Skewness and kurtosis, which describe the shape of the probability distribution, may vary by the sigma value. If sigma is too small, the convolution area between time required and time available is too small to use the resulting HFP in PSA; even if the value can be calculated, it will be out of the range generally considered in HRA (HFP = 1.0E-2 – 1.0E-3).

To derive a maximum acceptable value of HFP, Approach 2 is used to optimize sigma, which simply changes the μ of the lognormals while maintaining the sigma values. The mean of the lognormals is expressed by $e^{\mu+\frac{\sigma^2}{2}}$, where X ~ Log (μ, σ^2). To reflect the $T_{SAG\#_a}$ and $T_{SAG\#_v}$ of each SAG in the distribution of SAG diagnosis and decision, the mean of the lognormals of $T_{SAG\#\_d}$ was shifted by the summation of $T_{SAG\#_a}$ and $T_{SAG\#\_v}$. When applied to the original sigma value, a linear (simple) equation is created and the μ value is found. The difference between the two methods for RCS high pressure (Case 1) is shown in Fig. 9.

Beyond these two proposed approaches, estimates of average sigma values with upper and lower bounds are also presented for the uncertainty analysis due to the theoretical misgivings described above. The sigma values were estimated by the maximum likelihood technique, so the uncertainty of the curve fit increases as extrapolation is carried out. In this paper, the upper bound sigma was calculated by average sigma +1.64*(standard deviation of sigma samples) for the 90% percentile, while the lower bound sigma was calculated by average sigma −1.64*(standard deviation of sigma samples) for the 10% percentile. These sigma values were also applied to our model.

In Case 2-2, calculating the total time required is somewhat confusing since it represents that SAG-2 starts after only SAG-1 situational judgment and decision time has been completed; in other words, this case does not consider the time to complete SAG-1. In this case, the time of portable equipment transport and installation determines how many SAGs can be implemented over the given time period. To clarify the time integration, the various times required were compared, as depicted in Fig. 10. As a result, the time to conduct the overall SAG-02 with SAG-01 cognitive judgement is sufficient to be completed during the given time period ($T_{Transport\ and\ intallation}$), but it is insufficient to complete SAG-03 diagnosis and decision. Thus, the total time required in this case is approximated by the summation of $T_{Transport\ and\ intallation}$, T_{SAG03_d} and T_{SAG03_a}.

3.3. Distribution of time available

For calculating the HFP from delayed action when implementing SAG strategies, in addition to the total time required distribution, the total time available distribution is also needed. The MAAP 5.03

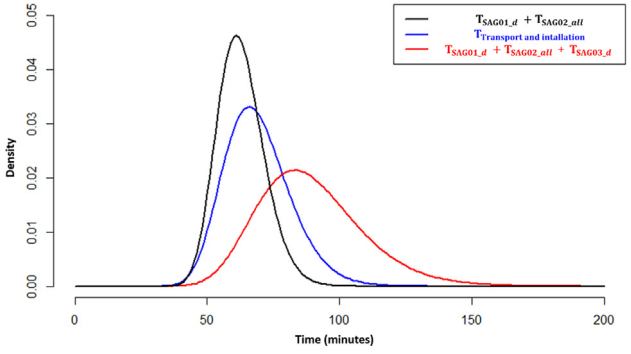

Fig. 10. Preliminary time analysis of RCS high pressure in Case 2-2.

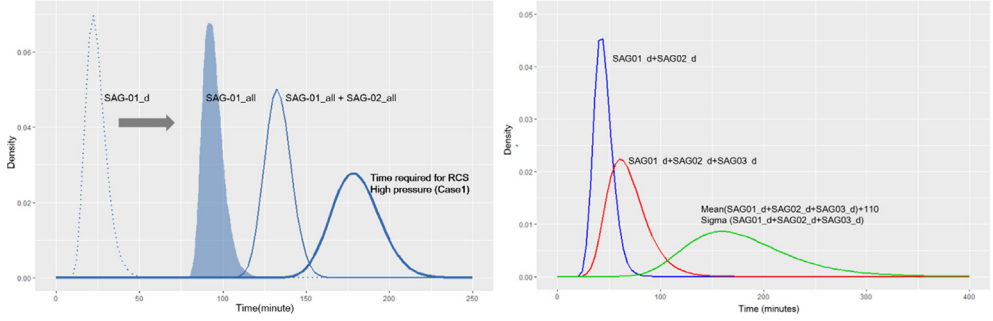

Fig. 9. Calculation process of Approach 1 (left) and Approach 2 (right) for RCS high pressure, Case 1.

code with parametric uncertainty analysis were used to determine the time available before RV failure considering phenomenological uncertainty. Ten important phenomena that affect RV failure were selected via screening analysis: decay heat generation, oxidation, in-vessel natural circulation, hot-leg natural circulation, cladding rupture, core collapse, flow area at collapsed core, lower plenum debris cooling, SG heat transfer, and RV Integrity. Each has several MAAP parameters that have default values and distributions of modeling parameters. Based on the parameter uncertainties, 80 scenarios were developed, for which the input data for MAAP calculation were sampled using the Latin hypercube sampling technique. The MAAP 5.03 code was run for the 80 cases considering uncertainty parameters related to RV failure, and intact RV probabilities were drawn out depending on the cases with different SAG strategies applied (e.g., RCS injection, SG injection). The results of intact RV probability depending on the mobile pump injection start time (hours) is shown in Fig. 11.

As depicted in Fig. 11, the simulation results represent not the form of probability density or cumulative distribution function, but the correlation between time and RV success probability [$p_{T_{available}}(t)$]. It is not easy to convert to the form of probability density distribution. Based on these results, the data was fitted into various types of graphs (i.e. log, exponential, polynomial function). In this case, P_{Fr} can be quantified by the following formula:

$$P_{Fr} = 1 - \int_0^c f_{T_{required}}(t)dt - \int_c^\infty f_{T_{required}}(t)\cdot p_{T_{available}}(t)dt$$
$$= \int_c^\infty f_{T_{required}}(t)\cdot p'_{T_{available}}(t)\,dt \quad (3)$$

where $p_{T_{available}}(t)$ is the success probability function from thermal-hydraulic results (intact RV probability), and $p'_{T_{available}}(t)$ is the failure probability function from fitting the dataset of 1-$p_{T_{available}}(t)$.

For quantifying $P_{Fr} = \int_c^\infty f_{T_{required}}(t)\cdot p'_{T_{available}}(t)\,dt$, the distribution of $p'_{T_{available}}(t)$ should be identified, so the datapoint from thermal-hydraulic results (intact RV probability) was extrapolated from the suitable type of graph. In the case of an RCS high pressure scenario, the distribution of $p'_{T_{available}}(t)$ is approximated by $0.0337\cdot e^{0.0114\cdot t}$ ($R^2 = 0.9399$), where c is 30 min. Applying this trend line to our method gives a probability of 1 at 300 min. This is because the uncertainty of the curve fit increases as extrapolation is carried out. Thus, P_{Fr} can be carefully estimated by the following formula: $P_{Fr} = \int_{30}^{300} f_{T_{required}}(t)\cdot p'_{T_{available}}(t)\,dt + \int_{300}^{\infty} f_{T_{required}}(t)\,dt$.

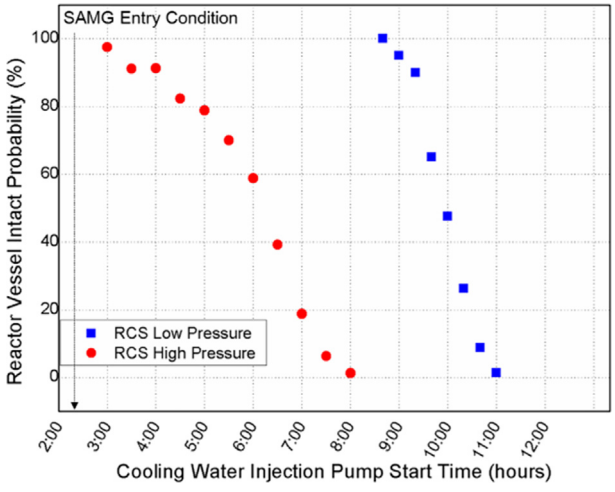

Fig. 11. Intact RV probability depending on mobile pump injection start time in RCS low and high pressure scenarios.

3.4. Comparison of the results from point estimation and proposed methods'

From Eq. (3) and the results obtained through the preceding sections, the overall HFP from delayed action when implementing SAG strategies (P_{Fr}) is in the range of 1.3E-01 to 4.3E-01. In other words, the probability that the SAG strategies would be successful is equal to a value between 0.57 and 0.87 in our models.

An uncertainty analysis was then performed to know the probability changes according to variance in mu and sigma of the total time required by the TSC to implement SAG strategies in RCS high pressure cases. Three cases were compared, as shown in Table 2. In the second section of the table (Proposed Method: Approach 1), the failure probability is similar to the values obtained from lower and upper bound sigma, with value differences of about 0.05. The extent of uncertainty in the crew response time is very similar, as the error factor (EF) is approximately 1.2 in all cases. Here, lognormal EF means how much higher a variable's upper bound is relative to the point estimate value of that variable, or it represents the ratio of 95% sigma and average sigma. The EF is expressed as $\sigma = \ln(EF)/1.645$. However, there are significant differences in the failure probabilities calculated from HCR/ORE generic sigma compared to TTX sigma. Determining sigma has been identified as an important aspect for calculating time reliability. It is not easy to classify SAM strategy actions into the previously defined three types of human interactions (CP1, CP2, and CP3 from EPRI [9]). When applying these sigma values into our dataset, the P_{Fr} from HCR/ORE is up to twice the value from TTX sigma; this gap implies that another TSC simulator experiment project is needed for identifying the PWR sigma under the SAMG situation.

As shown in Table 2, the P_{Fr} in the models proposed in this paper comes out much smaller than the values by point estimation, showing that the existing method is too conservative, and that the proposed models represent a methodology that can derive more substantial values. For example, many P_{Fr} values were 1.0 as determined by the point estimation method; in these cases, the P_{Fr} value should be obtained again by a complementary method using CBDTM or THERP, since this value cannot be applied directly to PSA models as the effect of the P_{Fr} value is relatively too great. If applied, for example, to Level 2 PSA, it would potentially cause the large early release frequency value to take a large portion.

There are also differences between the models this study proposed. Comparing Approach 1 and Approach 2, the values of P_{Fr} in the latter were higher than in the former. This is because the sigma value in Approach 2 was extracted as a larger value for the purposes of the underlying model. The larger the sigma value, the greater the thickness of the right tail portion of the lognormal distribution, thereby resulting in a difference in the P_{Fr} values of approximately 0.04. Although Approach 1 uses the exact value expressed by the formula implementing logarithmic characteristics, it may not be easy to accept, especially in places like regulatory bodies, because there is a big difference in the P_{Fr} values between point estimation and Approach 1 (about 0.7). However, more conservative values can be offered with Approach 2, so our methodology is meaningful to apply P_{Fr} values (same with HFP) into Level 2 PSA.

In addition to the sigma value, the median response time ($T_{1/2}$) as well is an important factor in calculating time reliability. The P_{Fr} values between the stress model and the other two models are

Table 2
Human failure probability from a delayed action (P_{Fr}) in the case studies.

	Point estimation: Approach 1					
	TTX average	TTX 10%	TTX 90%	PWR-CP1 (0.57)	PWR-CP2 (0.38)	PWR-CP3 (0.77)
RCS High Pressure (Case 1)	1.000	1.000	1.000	0.999	1.000	0.990
RCS High Pressure (Case 2-1)	1.000	1.000	1.000	1.000	1.000	0.995
RCS High Pressure (Case 2-2)	1.000	1.000	1.000	0.991	1.000	0.959
	Proposed Method: Approach 1					
RCS High Pressure (Case 1)	0.266	0.252	0.279	0.415	0.368	0.443
RCS High Pressure (Case 2-1)	0.422	0.415	0.474	0.527	0.514	0.532
RCS High Pressure (Case 2-2)	0.129	0.124	0.133	0.216	0.163	0.267
	Point estimation: Approach 2					
RCS High Pressure (Case 1)	1.000	1.000	1.000	0.999	1.000	0.988
RCS High Pressure (Case 2-1)	1.000	1.000	1.000	1.000	1.000	0.995
RCS High Pressure (Case 2-2)	1.000	1.000	1.000	0.990	1.000	0.958
	Proposed Method: Approach 2					
RCS High Pressure (Case 1)	0.304	0.284	0.324	0.415	0.368	0.443
RCS High Pressure (Case 2-1)	0.468	0.471	0.493	0.527	0.514	0.532
RCS High Pressure (Case 2-2)	0.133	0.126	0.139	0.216	0.163	0.267

almost twice as different. This indicates that the P_{Fr} value can be higher in real accident situations (SAMG entry condition) and also the importance of $T_{1/2}$. Ultimately, the proposed method may provide a means to complement the shortcomings of the existing methodology that cannot calculate time reliability over long periods, as previously mentioned in HCR/ORE [14]. In other words, even if the time window is longer in an actual SAMG situation, such as a progress time of at least 2 to over 24 h, our model can calculate the probabilities.

In the RCS high pressure scenarios, pre-activating F&B operation before entering SAMG is the best strategy to prevent RV failure. However, if F&B operation fails due to SDS valve failure, this study confirms that the value of P_{Fr} in Case 2-2 can be reduced by up to 30% compared to Case 2-1; recall that in Case 2-2 the SAG-02 RCS depressurization strategy can be performed in advance, whereas in Case 2-1 the SAGs are performed in sequence. This result is the same regardless of applying Approach 1 or Approach 2. Therefore, implementing RCS depressurization strategies in advance can be suggested as one SAMG improvement. It can also be seen that the value of P_{Fr} is controlled depending on the actual ERO ready time, and whether or not the portable equipment is prepared in advance before use. Depending on these two time factors, the value of P_{Fr} can be reduced by 60–70%. In other words, the results show that the ERO preparation time and the portable equipment preparation time should be as short as possible to prevent extreme situations in severe accidents, especially RV failure. To sum up, the following actions were shown here, in order, to play an important role in the success of strategy implementation: 1) F&B operation before SAMG entry, 2) quick preparation of portable equipment transport and installation, and ERO readiness, and 3) implementation of the SAG-02 strategy before waiting for portable equipment installation.

3.5. Application of performance shaping factors

In addition to sigma variability, time collected by TTX may contain numerous uncertainties due to the difference between experimental and real environments. According to post-interviews with participants, many felt less stressful than the extent of their experience with reactor trips would suggest. However, they agreed that the TSC would suffer from heavy workload and high stress levels in a real SAMG entry condition. In addition to stress level, various performance shaping factors (PSFs) are important factors for estimating P_{Fr}. A PSF is an aspect of a human's individual characteristics, the environment, organization, or task that specifically decreases or improves human performance, thus respectively increasing or decreasing the likelihood of human error [34]. Thus, some PSFs have to be considered in real SAMG situations.

The scenarios in our TTX simulation included several assumptions. First, it was assumed that there were no problems in diagnosing and identifying the problems, despite the experience level of the operators not being advanced. The second assumption was that the qualitative factors between the operators and the plant were well-established; for example, this may include an assumption that there were no abnormalities in the I&C to identify critical NPP parameters. The third was that the experiment was conducted in normal circumstances without any stress from time pressure or a poor environment. However, in an actual severe accident, many environmental factors surrounding TSCs will have serious effects, and the three above assumptions would likely change. Sensitivity analyses are therefore important to determine how the values of P_{Fr} change from scenario to scenario by considering PSFs that can reflect these situations.

The HCR model estimated crew median response times reflecting key plant- and task-specific PSFs (e.g., training level, man-machine interface quality). The model assumed that PSFs affect the response probability by changing the crew median response time (representing distribution location) but not the variability in response time (representing distribution shape). Hannaman et al. [35,36] suggested Eq. (4) for the application of a PSF coefficient into median response time:

$$T_{1/2} = n \times (1 + k_1) \times (1 + k_2) \times (1 + k_3). \quad (4)$$

This represents the allowable time in which the operator must take action to correctly resolve the situation. $T_{1/2}$ is the median response time, n is the nominal response time, k_1, k_2, k_3 are PSF coefficients, defined as follows: k_1 represents operator experience, with parameter values of Advanced (−0.22), Good (0), and Insufficient (0.44); k_2 represents stress level, with parameter values of Serious emergency (0.44), Heavy workload/Potential emergency (0.28), Excellent/Normal condition (0), and Vigilance problem (very low stress, 0.28); and k_3 represents operator/plant interface quality, with parameter values of Excellent (−0.22), Good (0), Sufficient (0.44), Poor (0.78), and Extremely poor (0.92). From Eq. (4) and the

Table 3
Scenario details including PSFs.

	k_1	k_2	k_3	Description
Scenario 1	0	0	0	Original TTX and stress data used
Scenario 2	0	0.44	0	Stress level of a real SAMG situation
Scenario 3	0.44	0.44	0	TSC with insufficient training/experience in a real SAMG situation
Scenario 4	−0.22	0.44	0	Veteran TSC in a real SAMG situation
Scenario 5	0	0.44	0.78	Poor quality I&C in a real SAMG situation
Scenario 6	0.44	0.44	0.92	Worst case

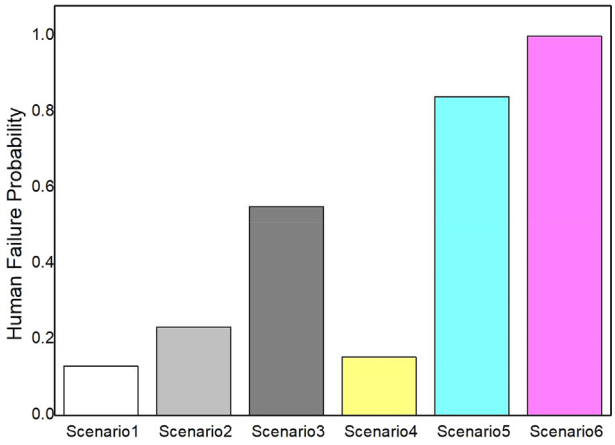

Fig. 12. Comparison of P_{Fr} values by scenario in RCS high pressure Case 2-2.

values suggested by the HCR model, the overall median response time in the current work was re-calculated for six scenarios, as defined in Table 3, with the P_{Fr} results of Case 2-2t shown in Fig. 12. The Case 2-2 was selected for its lower values of P_{Fr} obtained from simulation data.

As described in Table 3, Scenario 1 provides the baseline value of P_{Fr} with the same original TTX and stress data used. Scenario 2 represents only a high stress level in a serious emergency. Scenario 3 is the case that an insufficiently trained TSC conducts SAG strategies in a serious emergency situation, whereas Scenario 4 is that a well-trained TSC does so. Scenario 5 considers poor quality operator/plant interface in a serious emergency. Scenario 6 represents the worst case, adding to Scenario 3 an extremely poor I&C quality.

Comparing Scenarios 1, 2, 3, and 6, the P_{Fr} values in the RCS high pressure case change from 1.3E-1 to 9.9E-1. In Fig. 10, the optimal case has an HFP of 0.17 and the worst case has an HFP of almost 1. In the original scenario, HFP in the RCS high pressure case is low since the time required is shorter than the RV failure time. However, the time required is quite volatile, depending on environmental factors including I&C integrity and workload (stress level) as well as the extent of TSC and other staff training levels. This also indicates that the impact of PSFs is important, with each PSF having significant influences on the values of P_{Fr}. Results show that the effect of the type of PSFs on the value of P_{Fr} is very sensitive. Among the three considered factors, stress level has a 1.8 times impact on P_{Fr}. Operator experience has a 2.4 times impact, and the quality of operator/plant interface has a maximum of a 4.3 times impact on P_{Fr}. Thus, to reflect a real SAMG situation, the effects of various PSFs are essential to be considered for accurately calculating the time reliability.

Scenarios 3 and 4 demonstrate the importance of the TSC. Depending on TSC skill, HFP (P_{Fr}) varied from 1.5E-1 to 5.5E-1 in the RCS high pressure case. This implies that TSC training is highly important for accident mitigation, and also the possibility of zero HFP in a severe accident. Scenarios 3, 5, and 6 demonstrate the impact of operator/plant interface quality. The interval of failure probability increases significantly, and may represent the importance of interface quality in conducting the SAG-01 strategy, especially in SAG implementation ($T_{SAG\#\_a}$) and verification of effectiveness ($T_{SAG\#\_v}$). The sensitivity analysis results show that the effects of both TSC experience and the quality of the operator/plant interface in the RCS high pressure case are very sensitive.

4. Conclusion

This paper introduced an extended methodology for the estimation of human failure probability from delayed action (P_{Fr}) that occurs when the time required exceeds the time available. The approach can be classified into assessing the time required distribution and the time available distribution. The elements for identifying the time required distribution are as follows: 1) technical support center (TSC) diagnosis and decision time for each strategy, 2) emergency response organization (ERO) SAM strategy implementation time, 3) time to verify the effectiveness of the strategy, and 4) portable equipment transport and installation time. The time available distribution can be obtained by thermal-hydraulic code simulation (MAAP 5.03). The proposed approach was applied to TLOCCW case studies to evaluate overall SAM strategy implementation when the use of portable equipment is involved. As a result, the overall human failure probability from delayed action when implementing SAM strategies (P_{Fr}) was in the range of 1.3E-01 to 4.3E-01. In other words, the success probability of the SAM strategies against reactor vessel failure was equal to a value between 0.57 and 0.87 in our models.

Based on uncertainty and sensitivity analyses, the major findings and insights from the time analysis for SAMG HRA can be summarized as follows.

1) Due to the gap between the HCR/ORE generic sigma and our TTX sigma, determining sigma is an important aspect for calculating the time reliability of SAM strategy implementation. As the HCR/ORE sigma cannot be used for SAMG situations, additional data collection projects may be needed for identifying SAMG sigma.
2) The results from the proposed method are more realistic and appropriate than the point estimation method in evaluating SAM strategies using portable equipment. These realistic data can be applied to Level 2 PSA models as HFP data.
3) The value of P_{Fr} from Approach 2 was higher than from Approach 1 due to the large value of sigma. In addition to sigma, the median response time ($T_{1/2}$) is also an important factor in calculating P_{Fr} values. This fact was illustrated by the results of comparison between six scenarios that depended on PSFs.
4) Success of the SAM strategies depends on pre-action by the MCR before entering the SAMG condition, quick preparation of the ERO and portable equipment, and the order of the SAM strategies.
5) The sensitivity results showed that the effect of the type of PSFs on the value of P_{Fr} is very sensitive. Thus, in a real SAMG

situation, the effects of various PSFs should be considered for accurately calculating P_{Fr}.

6) Our model can be applied into Level 2 HRA as well SAMG HRA since it overcomes the shortcoming of the existing method by covering a longer time window.

Despite these promising findings, the current results should be discussed both from the point of view of uncertainty analysis and from the point of view of cognitive dependency.

Section 3.4 addressed the characterization of uncertainty in the sigma parameter of the TTX data. This uncertainty can be obtained in terms of confidence limits by standard statistical methods (i.e., R software package, 2019). Uncertainty in sigma may be produced by the choice of data-fitting process, with this paper adopting lognormal distributions to characterize uncertainty in the time reliability of our model. In addition to sigma though, the value of P_{Fr} is, in fact, the most sensitive to variations in median response time $T_{1/2}$.

An uncertainty measure on $T_{1/2}$ can be obtained using the FW or Monte Carlo sampling simulation methods. Propagation of the uncertainty of the parameters of the model, $T_{1/2}$ and sigma, can be performed easily only if the uncertainty is characterized by probability distributions. In this case, uncertainty in the value of P_{Fr} given by Eq. (3) can be obtained by Monte Carlo sampling from the distribution of total time required. Uncertainty values calculated in this way are likely to be large, particularly if the $T_{1/2}$ and sigma parameters were estimated on the basis of a small measurement sample (5 in this work). The estimates of P_{Fr} will inevitably have large uncertainty because of, in one case, the subjective nature of the estimates, and in the other, limited data.

Cognitive dependence [37] represents that success in the first of a series of cognitively dependent actions can imply a high likelihood of success in subsequent actions, whereas failure can imply an increased likelihood of failure in subsequent actions. This approach has the potential to be somewhat conservative, and a more analytical approach may prove to be worthwhile. To address the cognitive dependences in our study, a sensitivity analysis was performed, with results given in Table 4 for SAG-01 execution time.

In a severe accident progression, for example, the TSC does not know whether an indicator has failed or not. In this case, there are time uncertainties of execution time despite the successful diagnosis of SAG-01. Depending on how long it takes the TSC to recognize whether the indicator has failed or not, the execution time can increase from 50 min to 1–2 h. In Table 4, sensitivity results of P_{Fr} are described by changing the values of SAG-01 execution time. This result is important to know how different the P_{Fr} is by the timely success of SAG-01 execution. It can be seen that P_{Fr} increases with SAG execution time. This means that the timely success of SAG execution is likely to result in the success of the next SAG. This also implies the importance of cognitive dependence. While this problem of dependency should be considered tentatively, this study did not include this dependency. Since multiple teams work for mitigating accidents and focusing on the accident phenomenon, SAG failure due to indicator failures may be able to be recovered quickly.

Table 4
Sensitivity analysis of SAG-01 execution time for cognition dependence.

	SAG-01 execution time (min)				
	50	60	120	180	240
RCS High Pressure (Case 1)	0.266	0.290	0.591	0.990	1.000
RCS High Pressure (Case 2–1)	0.422	0.587	0.876	0.997	1.000
RCS High Pressure (Case 2–2)	0.129	0.129	0.129	0.129	0.129

In future studies, in addition to the TLOCCW event, further scenarios should be developed with more realistic data collection for TSC response times. Further, to validate the solidity of the logarithmic sigma in this paper, the number of data samples needs to be increased.

Despite these limitations and needs for further studies, the proposed method is suitable for SAMG HRA. The results from the proposed method are more realistic (i.e., not conservative) than other existing methods in evaluating SAM strategies involving the use of portable equipment. Results are also helpful to suggest an optimal order of strategy implementation for preventing reactor vessel or containment failure. In addition, this study demonstrates how the proposed time analysis method can be applied to evaluating human failure probabilities in overall HRAs as well as SAMG HRA.

Declaration of competing interest

The authors declare that they have no known competing financial interests or personal relationships that could have appeared to influence the work reported in this paper.

Acknowledgement

This research was supported by a Nuclear Research & Development Program of the National Research Foundation of Korea (NRF) grant, funded by the Ministry of Science and ICT (MSIT) (Grant Code: 2017M2A8A4015291).

References

[1] D.A. Topmiller, J.S. Eckel, E.J. Kozinsky, Human Reliability Data Bank for Nuclear Power Plant Operations (NUREG/CR-2744, vol. 1, US Nuclear Regulatory Commission, Washington, DC, USA, 1982.
[2] J. Reason, Human Error, Cambridge University Press, New York, USA, 1990.
[3] P. Moieni, A.J. Spurgin, A. Singh, Advances in human reliability analysis methodology. Part I: Frameworks, models and data, Reliab. Eng. Syst. Saf. 44 (1) (1994) 27–55.
[4] J. Kim, J. Cho, Technical challenges in modeling human and organizational actions under severe accident conditions for Level 2 PSA, Reliab. Eng. Syst. Saf. 194 (2020) 106239, 2020.
[5] V.N. Dang, G.M. Schoen, B. Reer, Overview of the modeling of severe accident management in the Swiss probabilistic safety analyses, in: Workshop Proceedings of ISAMM 2009: Implementation of Severe Accident Management Measures, 2010.
[6] V. Fauchille, H. Bonneville, J.Y. Maguer, Experience feedback from Fukushima towards human reliability analysis for level 2 probabilistic safety assessments, in: International Conference on Probabilistic Safety Assessment and Management (PSAM 12), June, Honolulu, Hawaii, 2014, June.
[7] N. Siu, D. Marksberry, S. Cooper, K. Coyne, M. Stutzke, PSA technology challenges revealed by the Great East Japan earthquake, in: PSAM Topical Conference in Light of the Fukushima Dai-Ichi Accident Tokyo, Japan, 2013, April.
[8] J. Kim, et al., Level 2 HRA: A SAMG-Based Detailed HRA Method, KAERI/TR-8118/2020, Korea Atomic Energy Research Institute (KAERI), 2020.
[9] Institute of Electrical and Electronics Engineers, in: Conference Record of the 1981 IEEE Standards Workshop on Human Factors and Nuclear Safety. Myrtle Beach, SC, USA, August/September 1981, IEEE Catalog No. TH0098-4, 1982.
[10] G.W. Hannaman, A.J. Spurgin, Y.D. Lukic, Human Cognitive Reliability Model for PRA Analysis (EPRI RP 2170-3), Electric Power Research Institute, Palo Alto, CA, USA, 1984.
[11] G.W. Hannaman, A.J. Spurgin, Y.D. Lukic, A model for assessing human cognitive reliability in PRA studies, in: IEEE Third Conference on Human Factors and Power Plants, Monterey, CA, USA, 1985.
[12] V. Joksimovich, et al., EPRI operator reliability experiments program: Model development/testing, in: Proceedings PSA '89, International Topical Meeting on Probability, Reliability and Safety Assessment, American Nuclear Society, La Grange Park, IL, USA, 1989.
[13] G.W. Parry, B.O.Y. Lydell, A.J. Spurgin, P. Moieni, A. Beare, An Approach to the Analysis of Operator Actions in Probabilistic Risk Assessment, EPRI Report TR-100259, 1992.
[14] A.J. Spurgin, et al., Operator reliability experiments using power plant simulators, in: Executive Summary and Technical Report (EPRI NP-6937), vols. 1 and 2, Electric Power Research Institute, Palo Alto, CA, USA, 1990.
[15] J. Kim, J. Ha, The evaluation of accident management strategy involving operator action, Nucl. Eng. Technol. 29 (5) (1997) 368–374.

[16] U.S. Nuclear Regulatory Commission and Electric Power Research Institute, An Integrated Human Event Analysis System (IDHEAS) for Nuclear Power Plant Internal Events At-Power Application, vol. 1, March 2017. NUREG-2199.
[17] B. Kirwan, L.K. Ainsworth, A Guide to Task Analysis: the Task Analysis Working Group, CRC, 1992.
[18] W. Jung, J. Kim, J. Park, Level 2 HRA: SAMG Scoping HRA Method, KAERI/TR-7651/2019, 2019.
[19] Nuclear Energy Institute, Crediting Mitigating Strategies in Risk-Informed Decision Making, NEI-16- 06, August 2016.
[20] P. Sobkowicz, M. Thelwall, K. Buckley, G. Paltoglou, A. Sobkowicz, Lognormal distributions of user post lengths in Internet discussions-a consequence of the Weber-Fechner law? EPJ Data Sci. 2 (1) (2013) 2.
[21] M.L. Delignette-Muller, C. Dutang, fitdistrplus: An R package for fitting distributions, J. Stat. Software 64 (4) (2015) 1–34.
[22] R.B. D'Agostino, M.A. Stephens, Goodness-of-Fit Techniques, in: Statistics: Textbooks and Monographs, 68, Marcel Dekker, Inc, New York, 1986.
[23] S. Asmussen, L. Rojas-Nandayapa, "Asymptotics of sums of lognormal random variables with Gaussian copula" (PDF), Stat. Probab. Lett. 78 (16) (2008) 2709–2714, https://doi.org/10.1016/j.spl.2008.03.035.
[24] X. Gao, Asymptotic behavior of tail density for sum of correlated lognormal variables, Int. J. Math. Math. Sci. (2009) 1–28, https://doi.org/10.1155/2009/630857, 2009.
[25] N.B. Mehta, J. Wu, A.F. Molisch, J. Zhang, Approximating a sum of random variables with a lognormal, IEEE Trans. Wireless Commun. 6 (7) (2007) 2690–2699.
[26] L.F. Fenton, The sum of lognormal probability distributions in scatter transmission systems, IRE Trans. Commun. Syst. CS-8 (1960) 57–67.
[27] C.F. Lo, WKB approximation for the sum of two correlated lognormal random variables, Appl. Math. Sci. 7 (128) (2013) 6355–6367.
[28] S.B. Slimane, Bounds on the distribution of a sum of independent lognormal random variables, IEEE Trans. Commun. 49 (2001) 975–978.
[29] Z.I. Botev, P. L'Ecuyer, Accurate computation of the right tail of the sum of dependent lognormal variates, arXiv:1705.03196, in: 2017 Winter Simulation Conference (WSC). 3rd–6th Dec 2017 Las Vegas, IEEE, NV, USA, 2017, ISBN 978-1-5386-3428-8, pp. 1880–1890, https://doi.org/10.1109/WSC.2017.8247924.
[30] Accessed December 14, 2011 R Development Core Team, R project R Foundation for Statistical Computing, Available at:, in: R: A Language and Environment for Statistical Computing, 2011 http://www.R-project.org/2011.
[31] B.P. Sangal, A.K. Biswas, The 3-parameter lognormal distribution and its applications in hydrology, Water Resour. Res. 6 (2) (1970) 505–515.
[32] E.L. Crow, K. Shimizu, Lognormal Distributions: Theory and Applications, Marcel Dekker, New York, 1988, p. 387pp.
[33] P.C. Bürkner, E. Charpentier, Modeling Monotonic Effects of Ordinal Predictors in Regression Models, 2018.
[34] H.S. Blackman, D.I. Gertman, R.L. Boring, Human error quantification using performance shaping factors in the SPAR-H method, in: 52nd Annual Meeting of the Human Factors and Ergonomics Society, 2008.
[35] G.W. Hannaman, A.J. Spurgin, Y.D. Lukic, Human Cognitive Reliability Model for PRA Analysis. Draft Report NUS-4531, EPRI Project RP2170-3. 1984, Electric Power and Research Institute, Palo Alto, CA, 1984.
[36] G.W. Hannaman, D.H. Worledge, Some developments in human reliability analysis approaches and tools, Reliab. Eng. Syst. Saf. 22 (1–4) (1988) 235–256.
[37] D.J. Wakefield, G.W. Parry, A.J. Spurgin, P. Moieni, Systematic Human Action Reliability Procedure (SHARP) Enhancement Project–SHARP1 Methodology Report, Electric Power Research Institute, 1992. EPRI TR-101711.